Two-Proton Radioactivity of ^{67}Kr

T. Goigoux,[1] P. Ascher,[1] B. Blank,[1] M. Gerbaux,[1] J. Giovinazzo,[1] S. Grévy,[1] T. Kurtukian Nieto,[1] C. Magron,[1] P. Doornenbal,[2] G. G. Kiss,[2] S. Nishimura,[2] P.-A. Söderström,[2] V. H. Phong,[2] J. Wu,[2] D. S. Ahn,[2] N. Fukuda,[2] N. Inabe,[2] T. Kubo,[2] S. Kubono,[2] H. Sakurai,[2,3] Y. Shimizu,[2] T. Sumikama,[2] H. Suzuki,[2] H. Takeda,[2] J. Agramunt,[4] A. Algora,[4,5] V. Guadilla,[4] A. Montaner-Piza,[4] A. I. Morales,[4] S. E. A. Orrigo,[4] B. Rubio,[4] Y. Fujita,[6,7] M. Tanaka,[6] W. Gelletly,[4,8] P. Aguilera,[9] F. Molina,[9] F. Diel,[10] D. Lubos,[11] G. de Angelis,[12] D. Napoli,[12] C. Borcea,[13] A. Boso,[14] R. B. Cakirli,[15] E. Ganioglu,[15] J. Chiba,[16] D. Nishimura,[16] H. Oikawa,[16] Y. Takei,[16] S. Yagi,[16] K. Wimmer,[3] G. de France,[17] S. Go,[18] and B. A. Brown[19]

[1]*Centre d'Études Nucléaires de Bordeaux Gradignan, Université de Bordeaux—UMR 5797 CNRS/IN2P3, Chemin du Solarium, 33175 Gradignan, France*
[2]*RIKEN Nishina Center, 2-1 Hirosawa, Wako, Saitama 351-0198, Japan*
[3]*Department of Physics, University of Tokyo, 7-3-1 Hongo, Bunkyo-ku, Tokyo 113-0033, Japan*
[4]*Instituto de Física Corpuscular, CSIC-Universidad de Valencia, E-46071 Valencia, Spain*
[5]*Institute of Nuclear Research of the Hungarian Academy of Sciences, P.O. Box 51, H-4001 Debrecen, Hungary*
[6]*Department of Physics, Osaka University, Toyonaka, Osaka 560-0043, Japan*
[7]*Research Center for Nuclear Physics, Osaka University, Ibaraki, Osaka 567-0047, Japan*
[8]*Department of Physics, University of Surrey, Guildford GU2 7XH, United Kingdom*
[9]*Comisión Chilena de Energía Nuclear, Casilla 188-D, Amunátegui 95, Santiago Centro, Santiago, Chile*
[10]*Institute of Nuclear Physics, University of Cologne, D-50937 Cologne, Germany*
[11]*Physik Department E12, Technische Universität München, D-85748 Garching, Germany*
[12]*Laboratori Nazionali di Legnaro dell'INFN, I-35020 Legnaro (Padova), Italy*
[13]*National Institute for Physics and Nuclear Engineering IFIN-HH, P.O. Box MG-6, Bucharest-Magurele, Romania*
[14]*INFN Sezione di Padova and Dipartimento di Fisica, Università di Padova, I-35131 Padova, Italy*
[15]*Department of Physics, Istanbul University, Istanbul 34134, Turkey*
[16]*Department of Physics, Tokyo University of Science, Noda, Chiba 278-8510, Japan*
[17]*Grand Accélérateur National d'Ions Lourds, B.P. 55027, F-14076 Caen Cedex 05, France*
[18]*Department of Physics and Astronomy, University of Tennessee, 401 Nielsen Physics Building, 1408 Circle Drive, Knoxville, Tennessee 37996-1200, USA*
[19]*Department of Physics and Astronomy, and National Superconducting Cyclotron Laboratory, Michigan State University, East Lansing, Michigan 48824-1321, USA*

(Received 19 May 2016; revised manuscript received 28 July 2016; published 14 October 2016)

In an experiment with the BigRIPS separator at the RIKEN Nishina Center, we observed two-proton ($2p$) emission from ^{67}Kr. At the same time, no evidence for $2p$ emission of ^{59}Ge and ^{63}Se, two other potential candidates for this exotic radioactivity, could be observed. This observation is in line with Q value predictions which pointed to ^{67}Kr as being the best new candidate among the three for two-proton radioactivity. ^{67}Kr is only the fourth $2p$ ground-state emitter to be observed with a half-life of the order of a few milliseconds. The decay energy was determined to be 1690(17) keV, the $2p$ emission branching ratio is 37(14)%, and the half-life of ^{67}Kr is 7.4(30) ms.

DOI: 10.1103/PhysRevLett.117.162501

Close to the valley of β stability, nuclear β decay, which is often associated with γ-ray emission, is the only decay mode possible. When moving closer to the limits of stability in both directions, the available decay energy, the Q value, increases at the same time as the binding energy of the excess particle decreases. Therefore, emission of β-delayed particles (protons, neutrons, or α particles) becomes more and more likely. Close to the proton drip line, β-delayed one-, two-, and (in particular recently) three-proton emission has been observed [1–6].

In all these cases, the excess protons are still sufficiently bound that direct particle emission is not possible. However, when moving further away from the line of stability, the protons are no longer bound by the strong nuclear force and the proton drip line is crossed. For slightly negative proton separation energies S_p or S_{2p}, β^+ decay can still compete with direct one- or two-proton emission; however, with separation energies typically below -1 MeV, one- and two-proton emission dominates for odd- and even-Z elements, respectively. We underline here that for $2p$ radioactivity, the one-proton separation energy has to be positive.

For odd-proton-number (odd-Z) elements, one-proton radioactivity is a well-established decay mode and is

observed for many nuclei between the tin and the lead regions [7]. This decay mode has been used to study the tunneling process, to determine the sequence of single-particle levels beyond the proton drip line, and to study the content of the nuclear wave function. One-proton radioactivity is a powerful tool to investigate nuclear structure beyond the limits of stability.

For even-Z and very light elements, the $2p$ emission process has a rather short half-life (of order 10^{-21} s), typically the time of a nuclear reaction. For medium-mass nuclei, half-lives in the millisecond range have been observed (see, e.g., [7,8]). The study of these nuclei started with the observation of $2p$ radioactivity in the decay of ^{45}Fe in experiments at Grand accélérateur national d'ions lourds (GANIL) [9] and Gesellschaft für Schwerionenforschung [10], followed by the observation of $2p$ radioactivity in the decay of ^{54}Zn in an experiment at GANIL [11]. The first evidence for $2p$ radioactivity of ^{48}Ni, based on a single event, was also obtained at GANIL [12]. Because of the implantation of the isotopes of interest in these experiments in silicon detectors, only the half-life, the $2p$ energy and the branching ratio for $2p$ emission could be observed. Nonetheless, this new decay mode was unambiguously identified by the absence of β radiation and the characteristics of the daughter decays after $2p$ emission for ^{45}Fe and ^{54}Zn.

These discovery experiments were followed by the direct observation of $2p$ radioactivity by means of time-projection chambers (TPCs) that allowed for an observation of the individual protons as well as the measurement of their energies and angles. The first of these experiments [13] (full analysis in [4]) was conducted at the LISE3 separator [14] of GANIL, where seven $2p$ events of ^{45}Fe were observed in the Bordeaux TPC [15]. An experiment conducted at Michigan State University with the Warsaw Optical Time-Projection Chamber [16] allowed the authors to gather much higher statistics for this nucleus and, thus, perform the first nuclear structure studies. The experiments with ^{54}Zn [17] and ^{48}Ni [18] complete the studies conducted up to now of medium-mass long-lived $2p$ emitters.

The comparison of experimental data with theoretical models has shown that, despite the limited statistics in many experiments and the shortcomings of the theoretical models presently available, first nuclear structure observables like the occupancy of orbitals could be extracted to some extent. Therefore, with improved experimental precision and new theoretical approaches, $2p$ radioactivity will potentially be a unique tool for nuclear physics beyond the proton drip line.

From mass and Q value predictions [19–23] from "local" mass models, it was shown that ^{59}Ge, ^{63}Se, and ^{67}Kr would be the next candidates for $2p$ radioactivity. Although the theoretical error bars were quite large (more than 200 keV for some of them, corresponding to a difference of about 2 orders of magnitude in Coulomb barrier penetration half-life), it was clear that ^{67}Kr would probably be the best candidate for $2p$ radioactivity (see Fig. 1) if one extrapolates from the measured Q values. One should keep in mind that higher Q values lead to shorter $2p$ half-lives and, therefore, to an increase of the $2p$ branching ratio compared to β decay.

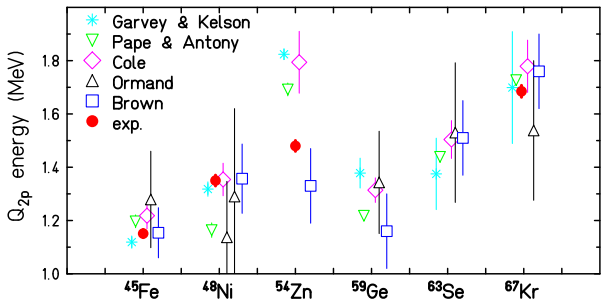

FIG. 1. The theoretical predictions of Q_{2p} values from different local-mass models [19–23] for the nuclei ranging from ^{45}Fe to ^{67}Kr are compared to experimental results where known. The experimental value for ^{67}Kr comes from the present Letter. Local mass models are based on properties for nuclei in the vicinity of the nucleus of interest, in contrast to global mass model predicting masses from, e.g., a Hartree-Fock-Bogoliubov microscopic interaction.

We used the BigRIPS separator [24,25] of the RIKEN Nishina Center to produce the isotopes of interest via the fragmentation of a high-intensity (up to 250 pnA) ^{78}Kr beam at 345 MeV/u. This beam impinged on a beryllium production target (thicknesses of 5 mm and 7 mm for different settings). The fragments were separated and selected by BigRIPS according to their magnetic rigidity, their energy loss in two aluminum degraders (2 mm at focal plane $F1$ and 2 mm at $F5$). The fragments of interest were identified by the BigRIPS standard detection setup consisting of a series of plastic scintillators, multisampling ionization chambers, and parallel-plate avalanche counters. Details of the identification procedure can be found in a recent paper [26].

The fragments thus selected and identified were transmitted to the exit of the ZeroDegree spectrometer (ZDS) [25] where a setup for decay studies was installed. It consisted of the WAS3ABi double-sided silicon strip detector (DSSSD) array [27] for implantation and detection of charged particles and the EURICA germanium detector array [28]. WAS3ABi consisted of three 1-mm-thick DSSSDs with 60 vertical (X) and 40 horizontal (Y) strips with a pitch of 1 mm. The gain was adjusted to a full range of about 5 MeV for the X strips and 10 MeV for the Y strips. WAS3ABi was calibrated in energy by means of conversion electrons from a ^{207}Bi source, and by the known β-delayed proton emitters ^{57}Zn, ^{61}Ge, and ^{65}Se produced in the present experiment. It had a resolution of 25 keV (FWHM) in X and 30 keV in Y.

EURICA is an array of 12 former EUROBALL cluster germanium detectors, each cluster detector containing seven crystals. It was mounted in close geometry around WAS3ABi and had a full-energy efficiency of about 8% at

TABLE I. Numbers of nuclei identified at the end of BigRIPS, at the end of the ZDS, and implanted in WAS3ABi.

Nucleus	BigRIPS	ZDS	WAS3ABi
^{59}Ge	1221	1162	562
^{63}Se	348	332	189
^{67}Kr	82	67	36

1.3 MeV. EURICA was calibrated with standard γ-ray sources.

In the present experiment, BigRIPS was optimized for four different settings relevant to the present Letter: (i) a setting on ^{51}Ni for WAS3ABi calibration, (ii) a setting on ^{65}Br to produce proton-rich nuclei, notably ^{59}Ge, ^{63}Se, and ^{67}Kr, (iii) a setting on ^{64}Se to study its decay characteristics, and (iv) a setting on ^{62}Se to search for the new isotopes ^{58}Ge and ^{62}Se (see [26] for details).

In Table I we give the numbers of nuclei identified at the exit of BigRIPS (focal plane $F7$), at the exit of the ZDS ($F11$), and of those implanted in the WAS3ABi array. From the measured sum, we obtain a transmission of 95% between the exit of BigRIPS and the exit of the ZDS. As the thickness of WAS3ABi was not enough to stop all fragments of interest, the matter layers at the exit of the ZDS were modified throughout the experiment to optimize the implantation of particular nuclei in the 3-mm-thick WAS3ABi array. The number of nuclei implanted in WAS3ABi was only about 50% of those identified. The correlation between events in BigRIPS, WAS3ABi, and EURICA was made by a common time stamp with a frequency of 10^8 Hz.

Each of the WAS3ABi strips was read out by a single electronic channel. With the gain settings mentioned above, it is evident that the electronics was saturated by implantation events. Moreover, not only did the implantation strip saturate, but the neighboring strips did as well. On average, 3.4 (4.3) strips were saturated on the X (Y) side for each implantation. However, each strip was also equipped with a timing channel that allowed the determination of the strip that fired first. The strip in which the implantation really took place is the fastest strip to fire. Therefore, the strip of implantation could be found by this means [27].

Finally, these implantation events in WAS3ABi were correlated in time with decay events taking place in the same strips where the implantation events were observed. This correlation allows one to establish decay-energy and time spectra for each nucleus. A similar time correlation was performed with events in EURICA running with a third independent data acquisition system.

The WAS3ABi dead time was determined with scalers for free and accepted triggers to be 22(2)%. The dead time per event that governs the percentage of events lost for short half-lives, when the data acquisition is still treating an implantation event while the decay takes place, was about 1.5 ms.

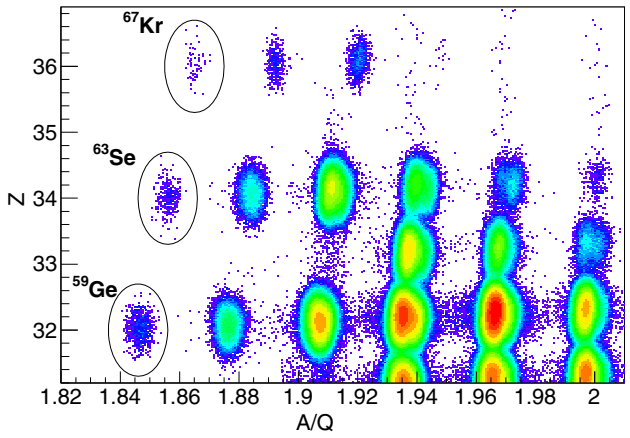

FIG. 2. Identification plot of the charge Z of the nuclides as a function of their ratio A/Q for isotopes produced in the setting optimized on ^{65}Br. The isotopes of interest are highlighted.

In the following, we will discuss the results obtained for ^{59}Ge, ^{63}Se, and ^{67}Kr. Figure 2 shows the isotopes implanted in WAS3ABi for the setting on ^{65}Br for which the correlation between implantation and decay could be performed.

The results obtained for the decay-energy spectra of the three nuclei as well as their decay-time curves are shown in Fig. 3. In our experiment, ^{59}Ge was mainly stopped in the third DSSSD, ^{63}Se in the second, and ^{67}Kr, due to its shorter range, in the first DSSSD.

Figure 3(a) shows all decay events correlated in time ($t < 100$ ms) and position with a ^{59}Ge implantation (in blue) and those in coincidence with β particles in neighboring detectors (in red). The decay energies are distributed over a wide range. In particular, at low energies, around 1.5–2.0 MeV, no pronounced peak is observed. This indicates that ^{59}Ge does not decay via a significant $2p$ branch, the upper limit being 0.2%, if we assume that all events but one come from β-delayed decays. All regions of the spectrum are in coincidence with β particles and the number of β-coincident events is in agreement with a β detection efficiency of about 65%.

From the expected energy, the pronounced structure around 6.5 MeV could originate from a $\beta 2p$ branch via the isobaric analogue state in ^{59}Ga. However, the present observation is certainly too vague to attribute this peak to a $\beta 2p$ decay. The half-life of ^{59}Ge was determined by correlating the implantation of this nucleus with subsequent decays [Fig. 3(b)]. A fit of decay events with an energy larger than 1 MeV (to cut events with only a β particle) with an exponential and a constant background yields a half-life value of 13.3(17) ms. This is close to the β-decay half-life predicted by the Gross theory [29] of 10.9 ms, and is indicative of a β-decay-dominated disintegration.

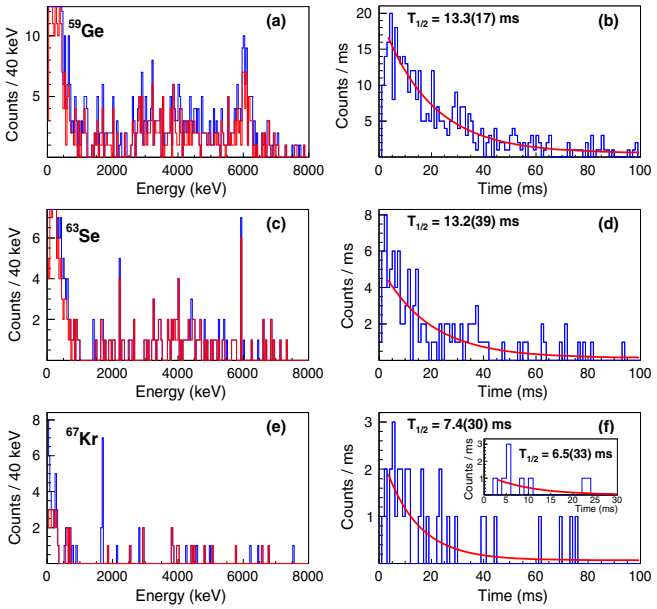

FIG. 3. Decay characteristics of (a),(b) ^{59}Ge, (c),(d) ^{63}Se, and (e),(f) ^{67}Kr with the charged-particle energy spectra on the left-hand side and the decay-time distributions of these nuclei on the right-hand side. For the charged-particle spectra, we show in blue all decay events and in red those decay events which are in coincidence with β-decay particles detected in neighboring detectors. The peak at 1690 keV for ^{67}Kr is due to $2p$ radioactivity. The inset in panel (f) is the half-life of ^{67}Kr determined from the events in the 1690-keV peak. For all half-life fits we excluded the first 3 ms due to dead-time losses and used only events with an energy above 1 MeV.

The results for ^{63}Se are similar [Figs. 3(c)–3(d)]. The decay energies are again distributed over a large energy range with very little structure. In the region of a possible $2p$ radioactivity, a peak with four counts is visible. However, three of these events are in coincidence with β particles detected in neighboring counters. The half-life, $T_{1/2} = 13.2(39)$ ms, is close to the Gross theory value of 13.4 ms, indicative of the decay being dominated by β decay. The $2p$ branch has an upper limit of 0.5% for this nucleus.

The decay-energy spectrum of ^{67}Kr is different from those of ^{59}Ge and ^{63}Se in that it exhibits a peak with nine events at low energy in the region where a $2p$ radioactivity peak would be expected. The peak is at $E = 1690(17)$ keV (with a standard deviation of the counts of 16 keV and a systematic uncertainty due to energy calibration of 5 keV) and we will show in the following that it indeed comes from $2p$ radioactivity of ^{67}Kr. The half-life is 7.4(30) ms as determined from all decay events for ^{67}Kr including daughter decays, where only the $2p$ daughter nucleus, ^{65}Se, contributes with a $2p$ branching ratio of 37(14)% (see below). If we use only the events with a decay energy in the 1690-keV peak, the procedure of Schmidt [30] yields $5.9^{+3.0}_{-1.5}$ ms when a correction for a 1.5-ms dead time is applied. Similarly, a maximum-likelihood fit of the spectrum conditioned by the $2p$ peak gives 6.5(33) ms. These values may be compared to the Gross theory prediction of 11.1 ms. The fact that the experimental half-life is shorter than the theoretical β-decay half-life indicates that the decay of ^{67}Kr proceeds most likely, as in the cases of ^{45}Fe, ^{48}Ni, and ^{54}Zn, via both decay channels, i.e., $2p$ radioactivity and β-delayed charged-particle emission.

The number of $2p$ decays observed has to be corrected for dead-time losses. As mentioned above, a general loss factor of 22(2)% comes from the dead time of the WAS3ABi data acquisition system, which leads to a corrected number of $2p$ decays of 11.5(39). However, as the data acquisition system has a dead time of 1.5 ms while it deals with an implantation event, we have 100% losses for the decay events arriving during this time span. This has little effect for decays with long half-lives but leads to significant losses of decay events for short-lived activities such as ^{67}Kr. The correction factor amounts to 13^{+8}_{-3}% in the present case. With these corrections, we determine a total number of $2p$ decays that we would have observed without losses of 13.3(45) events. With the number of implantations, we determine thus a $2p$ branching ratio of 37(14)%, yielding a partial $2p$ half-life of 20(11) ms.

In order to investigate the nature of the 1690-keV peak, we searched for β-decay radiation in neighboring detectors in coincidence with this peak. No signal above the pedestals was found. Figure 3(e) shows, in red, the first decay events of ^{67}Kr which are in coincidence with β radiation in neighboring detectors. No event in the peak region fulfils this condition. If we generate a spectrum of the signals in all neighboring detectors for decay events of ^{67}Kr other than the 1690-keV peak, we obtain the blue spectrum in Fig. 4. We overlay this spectrum with the β-decay radiation observed for ^{61}Ge, a known βp emitter, under similar conditions. Both spectra have the same shape. For an

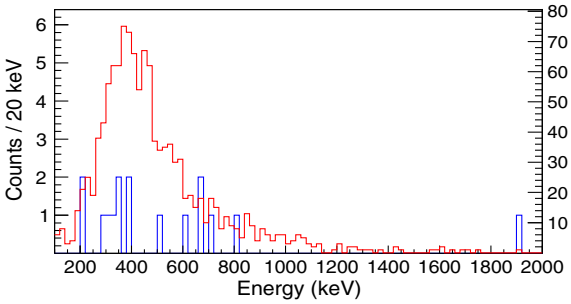

FIG. 4. Blue line (left Y axis): Spectrum observed in neighboring detectors in coincidence with the decay events outside of the 1690-keV peak for ^{67}Kr; i.e., if implantation and decay are observed in, e.g., DSSSD 1, we use here the signals observed in DSSSD 2 and 3. The β particles in coincidence with these events are visible. Red line (right Y axis): Same spectrum obtained under the same conditions for the well-known βp emitter ^{61}Ge with higher statistics.

implantation in a given DSSSD, we determined the β-detection efficiency for the two other DSSSDs to be 53(1)%, 92(1)%, and 51(1)% for an implantation in DSSSD1, DSSSD2, and DSSSD3, respectively. For ^{67}Kr (6 $2p$ events in DSSSD1, 3 in DSSSD2) this yields a β-detection efficiency of 67(1)%. Therefore, the probability that the events in the 1690-keV peak have a β particle in coincidence and that we miss all of them in our setup is as small as 5.5×10^{-6}.

We also checked the signals from EURICA. No 511-keV annihilation or other photon was observed in coincidence with the 1690-keV peak. Because we had an efficiency of 12% for a 511-keV γ ray, we derive a probability of 8.5% to miss all γ rays from positron annihilation.

We have accumulated sufficient evidence to claim that ^{67}Kr is a new ground-state two-proton emitter: (i) the experimental $2p$ decay energy of 1690(17) keV is well within the range of theoretical prediction (see Fig. 1); (ii) the half-life is shorter than the predicted β-decay half-life from the Gross theory; (iii) no β or γ radiation is observed in coincidence with the 1690-keV peak, whereas this radiation is observed in coincidence with other decays of ^{67}Kr.

From the plot of Grigorenko *et al.* [31], we determine a three-body half-life of 13.5 s for the f^2 configuration and 0.28 s for the p^2 configuration for an energy of 1.690 MeV. So, even if we assume a pure p^2 decay with a calculated half life of 0.28 s, the experiment is a factor of almost 40 shorter.

The shell model provides a good description of the nuclei in this mass region. With effective charges of $e_p = 1.5$ and $e_n = 0.5$ used for other pf shell nuclei [32], the calculated quadrupole moment of the mirror nucleus ^{67}Ga is $21.3e$ fm^2 compared to the experimental value of $19.5(5)e$ fm^2. The calculated $B(E2)$ for ^{66}Ge is $296e^2$ fm^4 compared to the experimental value of $268(22)e^2$ fm^4. The calculated energy of the first excited 2^+ state in ^{66}Ge is 1.03 MeV compared to the experimental value of 0.96 MeV.

For the theoretical interpretation of ^{67}Kr, we assume a ground-state spin and parity of $I^\pi = 3/2^-$ based on the ground-state spin and parity of the mirror nucleus ^{67}Ga. As in the mirror, we use $I^\pi = 3/2^-$ for the ground state of ^{65}Se. This leads to an $L = 0$ $2p$ decay from a $3/2^-$ state to a $3/2^-$ final state. The two-nucleon transfer amplitudes (TNAs) for $2p$ decay were calculated in a $1p - 0f$ shell-model space with the GXPF1A Hamiltonian [33]. The configurations allow for up to two proton or neutron holes in the $0f_{7/2}$ orbital. The calculated two-proton transfer amplitudes are 0.156 for the $0f_{7/2}$, 0.820 for the $0f_{5/2}$, 0.419 for the $1p_{3/2}$, and 0.371 for the $1p_{1/2}$ configurations, respectively.

The fractionation between p and f orbitals indicates that the one-orbital model of Grigorenko *et al.* [31] is incomplete. A more complete model should include the shell-model TNA that would take into account the two nucleon correlations. It is well known that the pairing correlations contained in the TNA strongly enhance the cross sections for two-nucleon transfer [34].

In summary, we have studied the decays of ^{59}Ge, ^{63}Se, and ^{67}Kr. In the case of the first two nuclei, a continuous decay-energy spectrum was observed, indicative of a β-delayed decay scheme. In the case of ^{67}Kr, the decay-energy spectrum exhibits a peak at 1690 keV which fulfills all of the criteria for $2p$ emission we could impose. It results in a 37(14)% $2p$ branch in the decay of ^{67}Kr. The present result opens the way for a detailed study of the $2p$ radioactivity of ^{67}Kr with a time-projection chamber. Such a study, which would yield angular and energy correlations for the two protons emitted, may shed light on the structure of ^{67}Kr. In particular, it might provide evidence for the influence of deformation on the $2p$ emission process and explain why the experimental half-life is much shorter than the shortest prediction from the Grigorenko model. However, to fully profit from such kinds of experimental results, theoretical models that include configuration mixing and deformation need to be developed.

This experiment was carried out under Programs No. NP0702-RIBF4R1-01, No. NP1112-RIBF82, and No. NP1112-RIBF93 at the RIBF operated by RIKEN Nishina Center, RIKEN and CNS, University of Tokyo. We would like to thank the whole RIBF accelerator staff for the support during the experiment and for maintaining excellent beam conditions with record intensities. This work was supported by the French-Japanese "Laboratoire international associé" FJ-NSP, by JSPS KAKENHI Grant No. 25247045, by the Istanbul University Scientific Project Unit under Project No. BYP-53195, by the Max-Planck Partner group and the Istanbul University Scientific Project Unit under Project No. YP-54135, by the NSF Grant No. PHY-1404442, by the UK Science and Technology Facilities Council (STFC) Grant No. ST/F012012/1, by the Japanese Society for the Promotion of Science under Grant No. 26 04808, by MEXT Japan under Grant No. 15K05104, and by the Spanish Ministerio de Economia y Competitividad under Grants No. FPA2011-24553 and No. FPA2014-52823-C2-1-P, Centro de Excelencia Severo Ochoa del IFIC SEV-2014-0398; Junta para la Ampliación de Estudios Programme (CSIC JAE-Doc contract) cofinanced by FSE.

[1] B. Blank and M. J. G. Borge, Prog. Nucl. Part. Phys. **60**, 403 (2008).
[2] K. Miernik *et al.*, Phys. Rev. C **76**, 041304 (2007).
[3] M. Pomorski *et al.*, Phys. Rev. C **83**, 014306 (2011).
[4] L. Audirac *et al.*, Eur. Phys. J. A **48**, 179 (2012).
[5] G. T. Koldste *et al.*, Phys. Rev. C **89**, 064315 (2014).
[6] A. A. Lis *et al.*, Phys. Rev. C **91**, 064309 (2015).

[7] B. Blank and M. Płoscajczak, Rev. Prog. Phys. **71**, 046301 (2008).
[8] M. Pfützner, M. Karny, L. V. Grigorenko, and K. Riisager, Rev. Mod. Phys. **84**, 567 (2012).
[9] J. Giovinazzo *et al.*, Phys. Rev. Lett. **89**, 102501 (2002).
[10] M. Pfützner *et al.*, Eur. Phys. J. A **14**, 279 (2002).
[11] B. Blank *et al.*, Phys. Rev. Lett. **94**, 232501 (2005).
[12] C. Dossat *et al.*, Phys. Rev. C **72**, 054315 (2005).
[13] J. Giovinazzo *et al.*, Phys. Rev. Lett. **99**, 102501 (2007).
[14] R. Anne and A. C. Mueller, Nucl. Instrum. Methods Phys. Res., Sect. B **70**, 276 (1992).
[15] B. Blank *et al.*, Nucl. Instrum. Methods Phys. Res., Sect. A **613**, 65 (2010).
[16] K. Miernik *et al.*, Phys. Rev. Lett. **99**, 192501 (2007).
[17] P. Ascher *et al.*, Phys. Rev. Lett. **107**, 102502 (2011).
[18] M. Pomorski *et al.*, Phys. Rev. C **83**, 061303 (2011).
[19] J. Jänecke and P. Masson, At. Data Nucl. Data Tables **39**, 265 (1988).
[20] A. Pape and M. Antony, At. Data Nucl. Data Tables **39**, 201 (1988).
[21] W. E. Ormand, Phys. Rev. C **55**, 2407 (1997).
[22] B. J. Cole, Phys. Rev. C **59**, 726 (1999).
[23] B. A. Brown, R. R. C. Clement, H. Schatz, A. Volya, and W. A. Richter, Phys. Rev. C **65**, 045802 (2002).
[24] T. Kubo, Nucl. Instrum. Methods Phys. Res., Sect. B **204**, 97 (2003).
[25] T. Kubo *et al.*, Prog. Theor. Exp. Phys. 03C003 (2012).
[26] B. Blank *et al.*, Phys. Rev. C **93**, 061301(R) (2016).
[27] S. Nishimura *et al.*, RIKEN Accel. Prog. Rep. **46**, 182 (2013).
[28] P.-A. Söderström *et al.*, Nucl. Instrum. Methods Phys. Res., Sect. B **317**, 649 (2013).
[29] T. Tachibana and M. Yamada, WWW Chart of the Nuclides 2014, http://wwwndc.jaea.go.jp/CN14/index.html.
[30] K. Schmidt, C.-C. Sahm, K. Pielenz, and H.-G. Clerc, Z. Phys. A **316**, 19 (1984).
[31] L. V. Grigorenko and M. V. Zhukov, Phys. Rev. C **68**, 054005 (2003).
[32] M. Honma, T. Otsuka, B. A. Brown, and T. Mizusaki, Phys. Rev. C **69**, 034335 (2004).
[33] M. Honma, T. Otsuka, B. A. Brown, and T. Mizusaki, Eur. Phys. J. A **25**, 499 (2005).
[34] C. Y. Wu, W. von Oertzen, D. Clinea, and M. W. Guidry, Annu. Rev. Nucl. Part. Sci. **40**, 285 (1990).